Low valent phosphorus in the molecular anions $[P_5Se_{12}]^{5-}$ and β-$[P_6Se_{12}]^{4-}$: phase change behavior and near infrared second harmonic generation†

In Chung,[ab] Joon I. Jang,[c] Matthew A. Gave,[a] David P. Weliky[a] and Mercouri G. Kanatzidis*[ab]

Received (in Berkeley, CA, USA) 17th September 2007, Accepted 11th October 2007
First published as an Advance Article on the web 12th November 2007
DOI: 10.1039/b714301j

The caesium salts of the novel molecular anions $[P_5Se_{12}]^{5-}$ and $[P_6Se_{12}]^{4-}$ are phase change materials and exhibit near infrared, non-linear optical second harmonic generation; $[P_5Se_{12}]^{5-}$ is a coordination complex with an octahedral P^{3+} center chelated by two $[P_2Se_6]^{4-}$ ligands whereas $[P_6Se_{12}]^{4-}$ features a $[P_2]^{4+}$ dimer chelated by two $[P_2Se_6]^{4-}$ ligands.

The structural diversity found in the chalcophosphate family is extensive. Various selenophosphate anions $[P_xQ_y]^{z-}$ (Q = S, Se) have been isolated and structurally characterized, for example, $[PSe_4]^{3-}$,[1] $[P_2Se_6]^{4-}$,[2] $[P_2Se_9]^{4-}$,[3] $[P_8Se_{18}]^{6-}$,[4] α-$[P_6Se_{12}]^{4-}$,[5] $^1_\infty[PSe_6^-]$[6] and $^1_\infty[P_2Se_6^{2-}]$.[7] The most common oxidation states of P in selenophosphates are P^{4+} and P^{5+}. Members of this family can exhibit the technologically important ferroelectric,[8] non-linear optical,[9] reversible redox chemistry relevant to secondary batteries,[10] photoluminescence,[11] and phase change properties.[12] Our investigations of alkali chalcophosphate compounds provided new insights into the relationship between the structure and the flux composition (A : P : Se ratio in the composition).[5] We also found that excess phosphorus in the flux helps to produce less oxidized $P^{2+/3+/4+}$ species such as $Rb_4P_6Se_{12}$[5] and $A_6P_8Se_{18}$ (A = K, Rb, Cs).[4] With this in mind, we focused on devising rational synthetic conditions to obtain P-rich species rather than the simple classical $[PSe_4]^{3-}$ or $[P_2Se_6]^{4-}$ anions. Here we describe the novel molecular $[P_5Se_{12}]^{5-}$ and β-$[P_6Se_{12}]^{4-}$ anions. The former includes P^{3+} and P^{4+} centers and features octahedrally coordinating P. The latter is a structural isomer of α-$[P_6Se_{12}]^{4-}$,[5] and it contains P^{2+} and P^{4+} centers. $Cs_5P_5Se_{12}$ and $Cs_4P_6Se_{12}$ exhibit reversible phase change behavior. Both crystalline and glassy $Cs_5P_5Se_{12}$ exhibit a second harmonic generation non-linear optical response.

The new compound $Cs_5P_5Se_{12}$‡ crystallizes in the non-centrosymmetric nonpolar space group $P\bar{4}$, Fig. 1a.§ It features the discrete molecular $[P_5Se_{12}]^{5-}$ anion with two types of formal charge, 3+ and 4+, on P, Fig. 1b. The trivalent formal charge is found on P(3) which is a central P atom chelated with two ethane-like $[P_2Se_6]^{4-}$ units to form a novel octahedral complex. The octahedral coordination of the trivalent P(3) atom is very unusual and features long bond distances, *e.g.* P(3)–Se(1) at 2.6606(8) Å and an even longer interaction of P(3)···Se(4) at 3.104(2) Å. The latter distance is much shorter than the 3.76 Å of the van der Waals radii sum.[13] The P(3)–Se(5) distance is normal at 2.349(2) Å, Fig. 1a. If the anion is to be viewed as a coordination complex, the P(3) atom plays the role of the metal and the formula can be expressed as $\{P[P_2Se_6]_2\}^{5-}$. P–Se bond distances in the chelating $[P_2Se_6]^{4-}$ ligands range from 2.121(2) to 2.280(2) Å. The $[P_2Se_6]^{4-}$ ligands in the molecule represent typical *anti*-type conformation but are distorted (see relevant angles in the ESI†).

It is noted that the bond angles for P(3) are close to 90° or 180°, Fig. 1. Deviation from 90° [Se(4)–P(3)–Se(4), 98.94(2); Se(4)–P(3)–Se(5), 80.22(3); Se(5)–P(3)–Se(5), 100.67(3)°] is caused by the μ_2-P(2). As a result, the octahedron around P(3) has excellent definition. The dihedral angle of Se(5)–Se(4)–Se(4)–Se(5) is only 2.35(2)° and indicates that the equatorial Se(2), Se(5), Se(5) and Se(2) atoms are nearly coplanar.

The $Cs_4P_6Se_{12}$‖ crystallizes in the monoclinic space group $P2_1/n$, Fig. 2a, b.** The compound features the new molecule β-$[P_6Se_{12}]^{4-}$, Fig. 2c. The central P_2 dimer is coordinated with two $[P_2Se_6]$ units to form a fulvalene-like skeleton. Both anion isomers α- and β-$[P_6Se_{12}]^{4-}$ consist of the central $[P_2]$ and two $[P_2Se_6]$ residues but they bind in a different fashion, Fig. 2. The β-species has a center of symmetry at the middle of the P(3)–P(3)′ bond and adopts the C_i point group. The formal charge on the P(3) atoms in the central $[P_2]$ unit is 2+. The P(3)–P(3)′ distance at 2.232(2) Å is slightly longer than the corresponding distance of 2.189(6) Å found in α-$[P_6Se_{12}]^{4-}$. α- and β-$[P_6Se_{12}]^{4-}$ were isolated as Rb^+ and Cs^+ salts, respectively, but it is unclear if the different

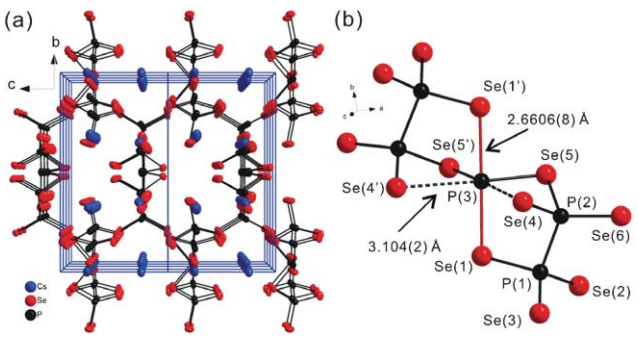

Fig. 1 (a) The non-centrosymmetric structure of $Cs_5P_5Se_{12}$. The thermal ellipsoids are shown with 60% probability. (b) $[P_5Se_{12}]^{5-}$ anion. Red solid line denotes long P–Se bonding at P(3)–Se(1), 2.6606(8) Å. Dashed lines indicate short P···Se nonbonding interaction at P(3)···Se(4), 3.104(2) Å.

[a]*Department of Chemistry, Michigan State University, East Lansing, MI 48824, USA*
[b]*Department of Chemistry, Northwestern University, Evanston, IL 60208, USA. E-mail: m-kanatzidis@northwestern.edu; Fax: +1 847 491 5937; Tel: +1 847 467 1541*
[c]*Department of Physics and Astronomy, Northwestern University, Evanston, IL 60208, USA*

† Electronic supplementary information (ESI) available: XPS, ^{31}P solid-state NMR, Raman, electronic absorption spectra, and selected bond distances and angles. See DOI: 10.1039/b714301j

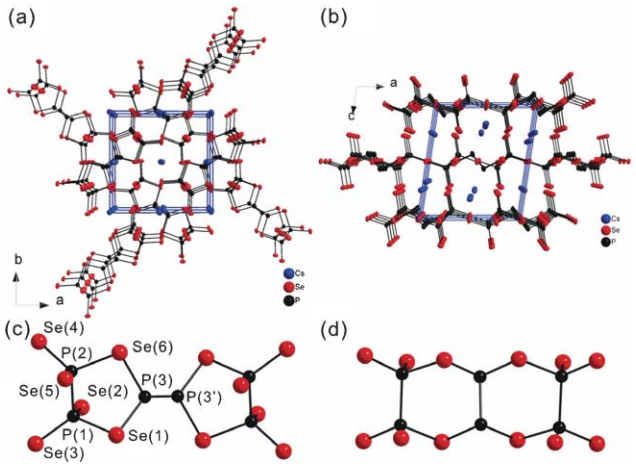

Fig. 2 Structure of $Cs_4P_6Se_{12}$ viewed down (a) the *c*-axis and (b) the *b*-axis. The thermal ellipsoids are shown with 60% probability. (c) The β-$[P_6Se_{12}]^{4-}$ anion and (d) the α-$[P_6Se_{12}]^{4-}$ anion for comparison.

structures are due to differences in packing forces associated with the alkali metal size.

Differential thermal analysis (DTA) of $Cs_4P_6Se_{12}$ performed at a rate of 10 °C min^{-1} showed a reversible crystal–glass phase transition, Fig. 3a. Upon heating the compound melted at 424 °C and upon cooling the melt solidified to a red glass. Only subsequent heating restored the crystals with an exothermic event at 263 °C followed by melting at 424 °C. A glass transition was observed at 204 °C for each cooling step. The amorphous nature of the glassy phase was confirmed with X-ray powder diffraction.

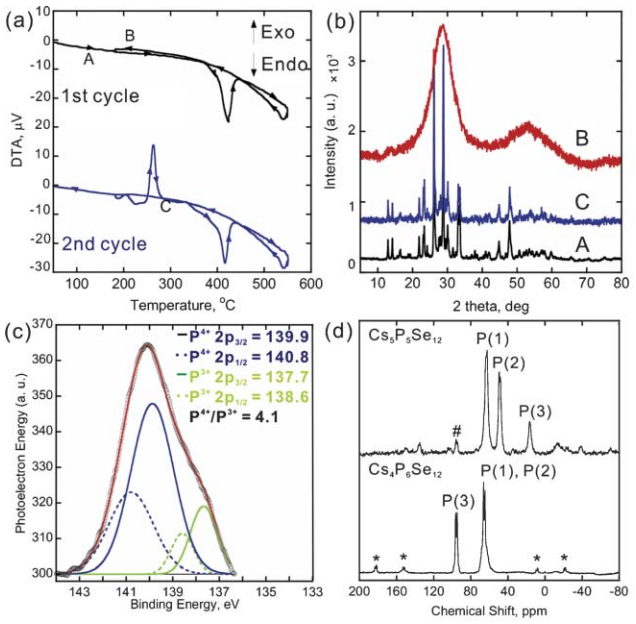

Fig. 3 (a) Differential thermal analysis diagrams of $Cs_4P_6Se_{12}$ showing melting in the 1st cycle with no crystallization on cooling (upper black line). Glass crystallization is observed in the 2nd heating cycle. $Cs_4P_6Se_{12}$ is a pristine crystal at A, glass at B and restored crystal at C. (b) X-Ray powder diffraction patterns of pristine (A), glass (B) and recrystallized crystal (C). (c) The X-ray photoelectron spectrum, peak fitting, and deconvolution profiles in the P 2p region of $Cs_5P_5Se_{12}$. (d) ^{31}P solid-state NMR spectra of $Cs_5P_5Se_{12}$ and $Cs_4P_6Se_{12}$ at a 14 kHz MAS frequency. * denotes spinning side bands and # $Cs_4P_6Se_{12}$ impurity.

The X-ray powder patterns after recrystallization were the same as those of pristine $Cs_4P_6Se_{12}$ indicating full recovery of the original crystal structure, Fig. 3b. Recrystallization and vitrification were reversible over many cycles. At cooling rates of 10 °C min^{-1} $Rb_4P_6Se_{12}$ did not form a glass suggesting that its glass crystallizes faster than that of $Cs_4P_6Se_{12}$. DTA of $Cs_5P_5Se_{12}$ at a rate of 10 °C min^{-1} exhibited a similar reversible phase transition behavior melting at 424 °C, forming a red glass at 250 °C and recrystallizing at 243 °C.

The Raman spectra of $Cs_5P_5Se_{12}$ display shifts at 219(s), 268(s), 349(w), 370(w), 478(w) and for $Cs_4P_6Se_{12}$ 221(s), 351(m), 368(m), 391(w), 447(w), 486(w) and 519(w) cm^{-1}. The spectra for both compounds were very similar. For $Cs_4P_6Se_{12}$, the shift at 221 cm^{-1} can be assigned to the P_2Se_6 stretching mode by comparison in the A_g stretching mode of D_{3d} symmetry of $[P_2Se_6]^{4-}$ ligand.[14] Other peaks at 486 and 519 cm^{-1} are also related to the P_2Se_6 fragment.[15] Peaks at 351 and 368 cm^{-1} were similarly observed in the spectrum of $Rb_4P_6Se_{12}$. The Raman spectra of glassy $Cs_5P_5Se_{12}$ and $Cs_4P_6Se_{12}$ showed broader and weaker peaks at 217, 349, and 368 cm^{-1} for the former and 218 and 358 cm^{-1} for the latter. These are at similar positions to those of the crystalline phase suggesting that the local structural motif is preserved in the glass, but crystallographic long range order is lost as seen in the X-ray powder diffraction patterns of glassy $Cs_5P_5Se_{12}$ and $Cs_4P_6Se_{12}$.

The X-ray photoelectron spectra of $Cs_5P_5Se_{12}$ and $Cs_4P_6Se_{12}$ confirmed the presence of two different oxidation states for P. For $Cs_5P_5Se_{12}$ peaks at higher energy (140.8, 139.9 eV) are assigned to P^{4+} centers, Fig. 3c. Peaks at 138.6 and 137.7 eV are assigned to P^{3+}. The XPS analysis revealed ratio of lower/higher oxidation state of P to be 4.1 and 1.9 for $Cs_5P_5Se_{12}$ and $Cs_4P_6Se_{12}$, respectively, which supported the structural analysis: $Cs_5[P^{3+}\{P^{4+}{}_2Se_6\}_2]$ and $Cs_4[(P^{2+})_2\{P^{4+}{}_2Se_6\}_2]$.

Solid-state ^{31}P NMR spectra of $Cs_5P_5Se_{12}$ and $Cs_4P_6Se_{12}$ were collected, Fig. 3d. The spectrum of $Cs_4P_6Se_{12}$ contained two doublets centered at 95.5 and 65.5 ppm with coupling constants of 250 and 270 Hz, respectively, with an approximately 1:2 intensity ratio. One possible assignment of these peaks is to the P^{2+} and P^{4+} atoms, respectively, with the splitting ascribed to two-bond P–P J-coupling. The spectrum of $Cs_5P_5Se_{12}$ could reasonably be assigned in a similar manner. A more detailed discussion of these assignments are given in supporting information.

The solid state electronic absorption spectra revealed sharp absorption edges for $Cs_5P_5Se_{12}$ and $Cs_4P_6Se_{12}$ at approximately the same energy of 2.17 eV, consistent with their orange color. The energy gap of the glassy phases were measured at 2.07 and 1.98 eV, respectively. The lower energy gaps of the glasses can be attributed to structural defects that create midgap states and band tailing.[16] A spectral shift in the absorption edge is a key feature in creating nonvolatile memory devices.[17]

Because of the non-centrosymmetric crystal structure of $Cs_5P_5Se_{12}$ and its good optical transparency from the edge of the energy gap to the mid-IR region, we investigated its second harmonic generation (SHG) response at room temperature. Using a modified Kurtz powder technique we measured polycrystalline samples of 45–63 μm size using 1200–2000 nm fundamental idler radiation from a tunable laser.[18] The SHG intensities obtained were compared with those of $LiNbO_3$ and $AgGaSe_2$, which are representative NLO materials for IR applications.[19] All samples were similarly prepared, and the same particle size range and

identical laser settings were used. The SHG intensity of $Cs_5P_5Se_{12}$ was approximately equal to that of $LiNbO_3$ and 25% that of $AgGaSe_2$.[20] As the particle size of $Cs_5P_5Se_{12}$ increased, the SHG intensity continuously decreased. Generally, when a powder sample is non-phase-matchable, SHG sensitivity peaks near the coherence length, which is typically 1–20 μm, and it starts to diminish through larger particle sizes. In this regard, $Cs_5P_5Se_{12}$ is type-I non-phase-matchable.[18] Despite this, such materials can be useful through 'random' quasi-phase-matching.[21]

Surprisingly, glassy $Cs_5P_5Se_{12}$ also exhibited a significant SHG response, at ~5% that of $AgGaSe_2$. There have been tremendous efforts to induce SHG in glasses because of the technological importance of their great transparency and formability, *e.g.* fabricating optical fibers.[22] It is possible that this is a rare example of observation of an SHG response from an amorphous material with no specific treatment such as thermal poling, electron beam irradiation and so on.[23] Since $Cs_5P_5Se_{12}$ is a phase change material and retains its local structural motif in the glassy state, as shown by Raman spectroscopy, we can expect the non-centrosymmetric arrangement to be partially preserved and plausibly give rise to some SHG response. Indeed, SHG of a glass sample was observed and X-ray powder diffraction patterns taken after the measurements still showed a predominantly amorphous nature for the sample. It cannot be completely ruled out, however, that idler beam-induced crystallization of the glass may be occurring or the existence of nanocrystals embedded in the glass matrix due to its phase change property. Further investigation of the glass thin film is in progress.

The results of this study demonstrate that novel chalcogenide species can be stabilized with reduced P^{3+} and P^{2+} atoms in the structure. Both compounds exhibit phase change behavior by forming glasses. The crystalline and glassy $Cs_5P_5Se_{12}$ showed a significant SHG response in the near infrared region of the spectrum.

Financial support from the National Science Foundation (Grant DMR-0702911 and 0306731 US/Ireland cooperation) and the Northwestern Materials Research Center under NSF (Grant DMR-0520513) for J.I.J. are gratefully acknowledged. I.C. would like to thank Dr G. S. Armatas for the help with the XPS measurement.

Notes and references

‡ Pure orange block-shaped crystals of $Cs_5P_5Se_{12}$ were obtained by heating a mixture of Cs_2Se : P : Se = 1 : 2.5 : 4 under vacuum in a silica tube at 400 °C for 3 d, followed by washing the product with degassed *N*,*N*-dimethylformamide (DMF) under a N_2 atmosphere to remove residual flux. The compound could also be obtained by direct combination reaction of starting materials at 400 °C for 3 d. Energy-dispersive spectroscopic (EDS) microprobe analysis showed an average composition of "$Cs_{4.8}P_5Se_{11.6}$". The single crystals are stable in DMF and alcohol and in air for several days.

§ Crystal data for $Cs_5P_5Se_{12}$ at 292(2) K: Siemens SMART Platform CCD diffractometer, Mo K_α radiation (λ = 0.71073 Å), $P\bar{4}$, a = 13.968(1) Å, c = 7.546(1) Å, V = 1472.2(3) Å^3, Z = 2, D_c = 3.986 g cm^{-3}, μ = 21.229 mm^{-1}, θ = 1.46–28.25°, 12701 total reflections, 3424 unique reflections with R(int) = 3.37%, refinement on F^2, GOF = 1.159, 73 parameters, R_1 = 3.00%, wR_2 = 7.27% for $I > 2\sigma(I)$, absolute structure parameter, 0.06(2). An empirical absorption correction was done using SADABS, and all atoms were refined anisotropically. CCDC 650231. For crystallographic data in CIF or other electronic format see DOI: 10.1039/b714301j

¶ADDSYM from the PLATON program (A. L Spek, *J. Appl. Crystallogr.* 2003, **36**, 7–13) were used for checking out higher symmetry.

‖ Pure orange block-shaped crystals $Cs_4P_6Se_{12}$ were obtained by heating a mixture of Cs_2Se : P : Se = 1 : 4 : 5 under the same conditions described above. EDS microprobe analysis showed an average composition of "$Cs_{3.8}P_6Se_{11.6}$". The glassy phase of $Cs_4P_6Se_{12}$ was prepared from melting single crystals of $Cs_4P_6Se_{12}$ under vacuum in a quartz tube at 800–900 °C for 1–2 min and quenching in ice water. The crystals are stable in DMF, alcohol and water and in air for several days.

** Crystal data for $Cs_4P_6Se_{12}$ at 100(2) K: STOE IPDS II diffractometer, Mo K_α radiation (λ = 0.71073 Å), $P2_1/n$, a = 10.836(1) Å, b = 10.5437(8), c = 12.273(1) Å, V = 1386.3(2) Å^3, Z = 2, D_c = 3.989 g/cm^3, μ = 21.309 mm^{-1}, θ = 2.33–29.99°, 8320 total reflections, 3961 unique reflections with R(int) = 5.95%, refinement on F^2, GOF = 1.077, 101 parameters, R_1 = 4.29%, wR_2 = 10.36% for $I > 2\sigma(I)$. An analytical and empirical absorption correction was done using XRED and XSHAPE, and all atoms were refined anisotropically. Structure solution and refinements for both compounds were performed with SHELXTL. CCDC 650232. For crystallographic data in CIF or other electronic format see DOI: 10.1039/b714301j

1 J. Garin and E. Parthe, *Acta Crystallogr., Sect. B*, 1972, **28**, 3672–3674.
2 R. H. P. Francisco, T. Tepe and H. Eckert, *J. Solid State Chem.*, 1993, **107**, 452–459.
3 K. Chondroudis and M. G. Kanatzidis, *Inorg. Chem.*, 1995, **34**, 5401–5402.
4 K. Chondroudis and M. G. Kanatzidis, *Inorg. Chem.*, 1998, **37**, 2582–2584.
5 I. Chung, A. L. Karst, D. P. Weliky and M. G. Kanatzidis, *Inorg. Chem.*, 2006, **45**, 2785–2787.
6 I. Chung, J. Do, C. G. Canlas, D. P. Weliky and M. G. Kanatzidis, *Inorg. Chem.*, 2004, **43**, 2762–2764.
7 I. Chung, C. D. Malliakas, J. I. Jang, C. G. Canlas, D. P. Weliky and M. G. Kanatzidis, *J. Am. Chem. Soc.*, DOI: 10.1021/ja075096c.
8 B. Scott, M. Pressprich, R. D. Willet and D. A. Cleary, *J. Solid State Chem.*, 1992, **96**, 294–300; C. D. Carpentier and R. Nitsche, *Mater. Res. Bull.*, 1974, **9**, 1097–1100.
9 R. Clement, P. G. Lacroix, D. Ohare and J. Evans, *Adv. Mater.*, 1994, **6**, 794–797.
10 A. Lemehaute, G. Ouvrard, R. Brec and J. Rouxel, *Mater. Res. Bull.*, 1977, **12**, 1191–1197; A. H. Thompson and M. S. Whittingham, *US Pat.*, 4 049 879, 1977.
11 Z. L. Huang, V. B. Cajipe, B. Lerolland, P. Colombet, W. J. Schipper and G. Blasse, *Eur. J. Solid State Inorg. Chem.*, 1992, **29**, 1133–1144.
12 J. D. Breshears and M. G. Kanatzidis, *J. Am. Chem. Soc.*, 2000, **122**, 7839–7840.
13 A. Bondi, *J. Phys. Chem.*, 1964, **68**, 441–451.
14 W. Brockner, L. Ohse, U. Pätzmann, B. Eisenmann and H. Schäfer, *Z. Naturforsch., A: Phys. Sci.*, 1985, **40**, 1248–1252; U. Pätzmann and W. Brockner, *Z. Naturforsch., A: Phys. Sci.*, 1987, **42**, 515–516.
15 J. A. Aitken, M. Evain, L. Iordanidis and M. G. Kanatzidis, *Inorg. Chem.*, 2002, **41**, 180–191.
16 G. A. Marking, J. A. Hanko and M. G. Kanatzidis, *Chem. Mater.*, 1998, **10**, 1191–1199; S. Dhingra and M. G. Kanatzidis, *Science*, 1992, **258**, 1769–1772.
17 T. Kyratsi, K. Chrissafis, J. Wachter, K. M. Paraskevopoulos and M. G. Kanatzidis, *Adv. Mater.*, 2003, **15**, 1428–1431; Y. Maeda, H. Andoh, I. Ikuta and H. Minemura, *J. Appl. Phys.*, 1988, **64**, 1715–1719; M. M. Maior, T. Rasing, S. W. H. Eijt, P. H. M. Vanloosdrecht, H. Vankempen, S. B. Molnar, Y. M. Vysochanskii, S. F. Motrij and V. Y. Slivka, *J. Phys.: Condens. Matter*, 1994, **6**, 11211–11220; J. B. Wachter, K. Chrissafis, V. Petkov, C. D. Malliakas, D. Bilc, T. Kyratsi, K. M. Paraskevopoulos, S. D. Mahanti, T. Torbrugge, H. Eckert and M. G. Kanatzidis, *J. Solid State Chem.*, 2007, **180**, 420–431.
18 S. K. Kurtz and T. T. Perry, *J. Appl. Phys.*, 1968, **39**, 3798–3813; J. P. Dougherty and S. K. Kurtz, *J. Appl. Crystallogr.*, 1976, **9**, 145–158.
19 D. N. Nikogosyan, *Nonlinear optical crystals: a complete survey*, Springer-Science, New York, 2005.
20 M. M. Choy and R. L. Byer, *Phys. Rev. B*, 1976, **14**, 1693–1706.
21 M. Baudrier-Raybaut, R. Haïdar, Ph. Kupecek, Ph. Lemasson and E. Rosencher, *Nature*, 2004, **432**, 374–376.
22 B. P. Antonyuk, *Opt. Commun.*, 2000, **181**, 191–195; B. P. Antonyuk and V. B. Antonyuk, *Opt. Commun.*, 1998, **147**, 143–147.
23 M. Fokine, K. Saito and A. J. Ikujima, *Appl. Phys. Lett.*, 2005, **87**, 171907; T. Fujiwara, M. Talahashi and A. J. Ikushima, *Appl. Phys. Lett.*, 1997, **71**, 1032–1034.

